

Role of Iron Uptake Systems in *Pseudomonas aeruginosa* Virulence and Airway Infection

Fabrizia Minandri,^a Francesco Imperi,^b Emanuela Frangipani,^a Carlo Bonchi,^a Daniela Visaggio,^a Marcella Facchini,^c Paolo Pasquali,^d Alessandra Bragonzi,^c Paolo Visca^a

Department of Sciences, Roma Tre University, Rome, Italy^a; Pasteur Institute-Cenci Bolognetti Foundation, Charles Darwin Department of Biology and Biotechnology, Sapienza University of Rome, Rome, Italy^b; Infections and Cystic Fibrosis Unit, Division of Immunology, Transplantation and Infectious Diseases, San Raffaele Scientific Institute, Milan, Italy^c; Department of Food Safety and Veterinary Public Health, Istituto Superiore di Sanità, Rome, Italy^d

Pseudomonas aeruginosa is a leading cause of hospital-acquired pneumonia and chronic lung infections in cystic fibrosis patients. Iron is essential for bacterial growth, and *P. aeruginosa* expresses multiple iron uptake systems, whose role in lung infection deserves further investigation. *P. aeruginosa* Fe³⁺ uptake systems include the pyoverdine and pyochelin siderophores and two systems for heme uptake, all of which are dependent on the TonB energy transducer. *P. aeruginosa* also has the FeoB transporter for Fe²⁺ acquisition. To assess the roles of individual iron uptake systems in *P. aeruginosa* lung infection, single and double deletion mutants were generated in *P. aeruginosa* PAO1 and characterized *in vitro*, using iron-poor media and human serum, and *in vivo*, using a mouse model of lung infection. The iron uptake-null mutant (*tonB1 feoB*) and the Fe³⁺ transport mutant (*tonB1*) did not grow aerobically under low-iron conditions and were avirulent in the mouse model. Conversely, the wild type and the *feoB*, *hasR phuR* (heme uptake), and *pchD* (pyochelin) mutants grew *in vitro* and caused 60 to 90% mortality in mice. The pyoverdine mutant (*pvdA*) and the siderophore-null mutant (*pvdA pchD*) grew aerobically in iron-poor media but not in human serum, and they caused low mortality in mice (10 to 20%). To differentiate the roles of pyoverdine in iron uptake and virulence regulation, a *pvdA fpvR* double mutant defective in pyoverdine production but expressing wild-type levels of pyoverdine-regulated virulence factors was generated. Deletion of *fpvR* in the *pvdA* background partially restored the lethal phenotype, indicating that pyoverdine contributes to the pathogenesis of *P. aeruginosa* lung infection by combining iron transport and virulence-inducing capabilities.

Pseudomonas aeruginosa is a leading cause of hospital-acquired infections and the main bacterial pathogen responsible for severe lung deterioration in cystic fibrosis (CF) patients. Among hospital-acquired *P. aeruginosa* infections, ventilator-associated pneumonia is a major clinical entity, with ≈20% prevalence and dramatically high mortality and monetary costs (1, 2). Other common syndromes associated with *P. aeruginosa* lung infection are those occurring in patients with chronic lung disease, such as chronic obstructive pulmonary disease and CF (3). All CF patients experience *P. aeruginosa* lung infection during their lifetime, and more than 80% of them become chronically infected in the adult years (3, 4). Lifelong *P. aeruginosa* infection causes decreases in lung function and poor clinical scores for CF patients, ultimately resulting in a fatal prognosis (5).

Like most bacterial pathogens, *P. aeruginosa* needs substantial amounts of iron to infect the host and multiply within tissues and body fluids. Under normal *in vivo* conditions, iron is not readily available due to sequestration in iron binding proteins, such as transferrin in serum and lactoferrin in mucosal secretions, which are components of the innate immunity and provide a forefront “nutritional” defense against invading pathogens (6). On the other hand, *P. aeruginosa* has an impressive capacity to retrieve iron from a variety of natural sources through a multiplicity of systems for the active transport of iron compounds into the cell (7, 8). First of all, *P. aeruginosa* produces two siderophores, pyoverdine and pyochelin, endowed with very different structural and functional properties, and both are capable of chelating ferric ions (Fe³⁺). Pyoverdine is a peptidic siderophore containing two hydroxamic groups and a fluorescent dihydroxyquinoline chromophore, which create a very efficient iron coordination center

(9–11), while pyochelin is a salicylate-based siderophore with a lower affinity for iron (12, 13). Both siderophores are actively translocated across the outer membrane upon binding to specific receptors, namely, the FptA and FpvA outer membrane proteins for pyochelin and pyoverdine transport, respectively (14). *P. aeruginosa* can also assimilate heme, which may be released by hemoproteins during infection, through the Has and Phu systems. While Phu accounts for direct heme uptake via the PhuR receptor, the Has system relies on a secreted hemophore protein, HasA, which catches heme and delivers it to the HasR outer membrane receptor (15). Translocation of all these iron carriers through the cognate receptor requires the consumption of the proton motive force by the TonB-ExbB-ExbD protein complex, which serves as an energy coupler for active transport across the outer membrane (16). While *P. aeruginosa* PAO1 carries three different *tonB* genes (*tonB1*, *tonB2*, and *tonB3*), *tonB1* has been demonstrated to play

Received 11 February 2016 Returned for modification 15 March 2016

Accepted 26 May 2016

Accepted manuscript posted online 6 June 2016

Citation Minandri F, Imperi F, Frangipani E, Bonchi C, Visaggio D, Facchini M, Pasquali P, Bragonzi A, Visca P. 2016. Role of iron uptake systems in *Pseudomonas aeruginosa* virulence and airway infection. *Infect Immun* 84:2324–2335. doi:10.1128/IAI.00098-16.

Editor: S. M. Payne, University of Texas at Austin

Address correspondence to Paolo Visca, paolo.visca@uniroma3.it.

Supplemental material for this article may be found at <http://dx.doi.org/10.1128/IAI.00098-16>.

Copyright © 2016, American Society for Microbiology. All Rights Reserved.

the main role in siderophore-mediated iron uptake (17–19). Additionally, the *P. aeruginosa* genome encodes more than 30 TonB-dependent outer membrane receptors, some of which are implicated in the uptake of xenosiderophores (i.e., siderophores produced by other microorganisms, such as ferrichrome or deferrioxamine) or other, still uncharacterized exogenous iron carriers (20, 21). In addition to TonB-dependent iron uptake systems, *P. aeruginosa* has the ability to acquire ferrous iron (Fe^{2+}) via the TonB-independent Feo system, whose main component is the FeoB permease, located in the cytoplasmic membrane and containing a cytosolic N-terminal domain with GTPase activity (22).

Active iron uptake is shut off in the presence of sufficient intracellular iron, and the Fur repressor protein sits atop the iron regulation hierarchy, sensing the intracellular levels of the corepressor Fe^{2+} and directly or indirectly repressing the transcription of almost all genes related to iron uptake (23, 24). Most of the *P. aeruginosa* iron uptake systems have a second level of regulation, resulting from autoinduction of iron uptake genes, which takes place when the iron carrier is effectively internalized by the cell (8, 21, 24). The best-studied autoregulatory system is the pyoverdine surface signaling cascade, in which ferripyoverdine binding to the FpvA receptor transmits a signal to the cytoplasm via the membrane-bound anti-sigma factor protein FpvR, which ultimately results in activation of both the FpvI and PvdS sigma factors. While the transcriptional specificity of FpvI is restricted to the *fpvA* receptor gene, the PvdS sigma factor governs, either directly or indirectly, the expression of several genes forming the PvdS regulon. These include pyoverdine biosynthetic genes as well as genes encoding major *P. aeruginosa* virulence factors, such as the PrpL protease and exotoxin A (25, 26). Thus, pyoverdine is predicted to have dual roles in *P. aeruginosa* virulence: (i) it provides bacteria with an essential nutrient for *in vivo* growth and (ii) it serves as a signal molecule for the expression of major virulence factors, which in turn may contribute to increased iron availability to bacteria during infection (21, 25).

The importance of iron for *P. aeruginosa* infection was first highlighted using an intraperitoneal mouse infection model (27), and pyochelin was shown to increase *P. aeruginosa* lethality during intraperitoneal infection (28). Thereafter, a number of studies were performed to ascertain the roles of individual *P. aeruginosa* siderophores in infectivity and virulence. Pyoverdine-deficient *P. aeruginosa* mutants were less virulent than the wild type in the burned-mouse model (29), and the PvdS sigma factor was demonstrated to play a prominent role in both rabbit endocardial infection and mouse lung infection (30, 31). However, intranasal inoculation into immunosuppressed mice revealed no significant difference in lethality at 48 h between wild-type PAO1 and the pyochelin- or pyoverdine-deficient mutant or the double mutant, though the mouse killing kinetics and bacterial counts in blood suggested that virulence and invasive capacity were attenuated in siderophore mutants (32). More importantly, it was shown that *tonB1* inactivation severely impaired the capacity of *P. aeruginosa* to multiply in the muscles and lungs of immunosuppressed mice (17), suggesting that active transport of ferric compounds is an essential component of the *P. aeruginosa* virulence armamentarium.

In this work, we compared the contributions of individual iron uptake systems to *P. aeruginosa* virulence by using a well-established mouse model of *P. aeruginosa* lung infection (33, 34). For this purpose, deletion mutants in the major iron uptake systems

were generated in *P. aeruginosa* PAO1, and their iron uptake and virulence phenotypes were characterized *in vitro* and *in vivo*. We demonstrated that *P. aeruginosa* thrives in an iron-poor environment in mouse lungs at the onset of infection and that individual iron uptake systems have different abilities to promote lethal disease in mice, according to the following hierarchy: pyoverdine > pyochelin > ferrous iron uptake \cong heme uptake. Our findings confirm that ferric iron uptake is essential for *P. aeruginosa* lung infection and provide novel *in vivo* evidence of the dual roles of pyoverdine as a primary siderophore and a virulence-inducing signal molecule.

MATERIALS AND METHODS

Bacterial strains, plasmids, and growth conditions. Bacterial strains and plasmids used in this work are listed in Table 1. *Escherichia coli* and *P. aeruginosa* were routinely grown in Luria-Bertani (LB) medium (35) or on LB agar plates for general genetic procedures. *P. aeruginosa* was grown in the following media for specific iron uptake assays: iron-depleted Bacto Casamino Acids (Becton Dickinson, Sparks, MD) medium (DCAA) (36), Trypticase soy broth (Neogen Co., Lansing, MI) dialysate medium (TSBD) (37), M9 minimal medium (31) supplemented with 0.2% glucose as the carbon source and 0.1 or 1.0 mM 2,2'-dipyridyl (DIP) (Sigma) as an iron chelator, and GGP medium (38). DCAA was supplemented with 1 mM NaHCO_3 for growth experiments in the presence of transferrin. Apo-transferrin (iron-free; Sigma) was dissolved in DCAA supplemented with 10 mM NaHCO_3 buffered at pH 7.5 with acetic acid to obtain a final concentration of 2.5 mg/ml, equivalent to 31.3 μM apo-transferrin (DCAA-Tf). For all the media used, iron-sufficient conditions were obtained by adding FeCl_3 or FeSO_4 to the indicated concentrations.

For mutant construction, *E. coli* and *P. aeruginosa* strains were grown in LB, with or without antibiotics, at 37 and 42°C, respectively, with vigorous aeration. For sucrose selection, LB containing 5% sucrose or LB containing 5% sucrose and 40 μM FeSO_4 was used. When required, antibiotics were added at the following concentrations for *E. coli*, with the concentrations used for *P. aeruginosa* shown in parentheses: ampicillin, 100 $\mu\text{g ml}^{-1}$; carbenicillin (250 $\mu\text{g ml}^{-1}$); chloramphenicol, 30 $\mu\text{g ml}^{-1}$ (375 $\mu\text{g ml}^{-1}$); gentamicin, 10 $\mu\text{g ml}^{-1}$ (200 $\mu\text{g ml}^{-1}$); nalidixic acid, 20 $\mu\text{g ml}^{-1}$; and tetracycline, 12.5 $\mu\text{g ml}^{-1}$ (100 $\mu\text{g ml}^{-1}$).

Genetic procedures. Unmarked in-frame deletion mutants in iron uptake genes were constructed by suicide plasmid insertion mutagenesis (39, 40). *E. coli* was used for recombinant DNA manipulations. The constructs for mutagenesis were generated by directional cloning into the pEX18Tc or pDM4 vector (Table 1) (39, 40) of two DNA fragments of ca. 600 bp, encompassing the regions upstream and downstream of the sequence to be deleted. Fragments were amplified by PCR, digested with the appropriate restriction enzymes, and cloned into pEX18Tc or pDM4, generating the derivative vectors pEX18Tc Δ feoB, pDM4 Δ hasR, pDM4 Δ phuR, pDM4 Δ tonB1, and pDM4 Δ fpvR (Table 1). PCR primers and restriction enzymes used for cloning of PCR products are listed in Table S1 in the supplemental material. All constructs were verified by DNA sequencing. Deletion vectors were conjugally transferred from *E. coli* S17-1 λ pir into the *P. aeruginosa* PAO1 wild type or into suitable deletion mutants to obtain the *hasR* *phuR*, *tonB1* *feoB*, and *pvdA* *fpvR* double mutants. The in-frame deletion mutations were obtained by recombination as described previously (39, 40). To allow the growth of *tonB1*-deficient strains, *tonB1* transconjugants were selected in the presence of 40 μM FeSO_4 , and both *tonB1* and *tonB1* *feoB* mutants were routinely maintained in medium supplemented with 40 μM FeSO_4 . All the deletion events were verified by PCR using primers flanking the deleted region.

The *pvdA*, *pchD*, *tonB1*, *hasR*, and *phuR* mutations were complemented *in trans* by supplying each coding sequence, along with the indigenous promoter region, on plasmid pUCP18 (41). DNA fragments were

TABLE 1 Bacterial strains and plasmids used in this study

Strain or plasmid	Genotype and/or relevant characteristics	Reference or source
Strains		
<i>P. aeruginosa</i> strains		
PAO1	ATCC 15692 (wild type, prototroph)	American Type Culture Collection
PAO1 PpvdA'-mCherry	Wild type with PpvdA::mCherry	This work
pvdA mutant	PAO1 Δ pvdA	45
pchD mutant	PAO1 Δ pchD	82
pvdA pchD mutant	PAO1 Δ pvdA Δ pchD	83
PAO1 pvdA pchD PpvdA'-mCherry	PAO1 Δ pvdA Δ pchD PpvdA::mCherry	This work
fpvR mutant	PAO1 Δ fpvR	This work
pvdA fpvR mutant	PAO1 Δ pvdA Δ fpvR	This work
pvdS mutant	PAO1 Δ pvdS Gm ^r	31
hasR phuR mutant	PAO1 Δ hasR Δ phuR	This work
feoB mutant	PAO1 Δ feoB	This work
tonB1 mutant	PAO1 Δ tonB1	This work
tonB1 feoB mutant	PAO1 Δ tonB1 Δ feoB	This work
toxA mutant	PAO1 <i>phoA</i> wp03q2B07 (mutant 40695)	Transposon mutant collection of University of Washington
<i>Escherichia coli</i> strains		
DH5 α	F' <i>recA1 endA1 hsdR17 supE44 thi-1 gyrA96 relA1</i> Δ (<i>lacZYA-argF</i>)U169 ϕ 80 <i>lacZ</i> Δ M15 Nal ^r	35
S17-1 λ pir	<i>recA thi pro hsdR</i> (M ⁺ RP4)::2-Tc::Mu::Km Tn7 λ pir Tp ^r Sm ^r	84
Plasmids		
pEX18Tc	Allelic exchange vector pMB1 replicon; <i>oriT</i> ⁺ <i>sacB</i> ⁺ <i>lacZ</i> α <i>mob</i> ⁺ Tc ^r	39
pDM4	Suicide vector; <i>sacBR oriR6K</i> Cm ^r	40
pmCherry-1	Vector used as template for amplification of the mCherry coding sequence	Clontech
Mini-CTX1	Promoter-probe vector; Ω -FRT-attP-MCS <i>ori int oriT</i> Tc ^r	42
pFLP2	FLP recombinase-expressing plasmid; Ap ^r	39
Mini-CTX1 mCherry	Tc ^r	This study
Mini-CTX PpvdA'-mCherry	Plasmid to insert a PpvdA-mCherry fusion into the chromosome of <i>P. aeruginosa</i> ; Tc ^r	This study
pDM4 Δ fpvR	pDM4 derivative carrying the flanking regions of the <i>fpvR</i> coding sequence	This study
pDM4 Δ hasR	pDM4 derivative carrying the flanking regions of the <i>hasR</i> coding sequence	This study
pDM4 Δ phuR	pDM4 derivative carrying the flanking regions of the <i>phuR</i> coding sequence	This study
pEX Δ feoB	pEX18Tc derivative carrying a Gm ^r -GFP cassette between the <i>feoB</i> flanking regions	This study
pDM4 Δ tonB	pDM4 derivative carrying the flanking regions of the <i>tonB1</i> coding sequence	This study
pMP220::PfeoA	pMP220 derivative carrying a PfeoA::lacZ transcriptional fusion; Tc ^r	31
pPZ-toxA	pPZ20 derivative carrying a PtoxA::lacZ translational fusion; Cb ^r	26
pPZ-prpL	pPZTC derivative carrying a PprpL::lacZ transcriptional fusion; Cb ^r	26
pUCP18	<i>E. coli</i> - <i>Pseudomonas</i> shuttle vector derived from pUC18; ColE1 pRO1600 Ap ^r Cb ^r	41
pUCPpvdA	pUCP18 derivative carrying the coding sequence of <i>pvdA</i> with its own promoter	This study
pUCPpchD	pUCP18 derivative carrying the coding sequence of <i>pchD</i> with its own promoter	This study
pUCPtonB1	pUCP18 derivative carrying the coding sequence of <i>tonB1</i> with its own promoter	This study
pUCPphuRhasR	pUCP18 derivative carrying the coding sequences of <i>phuR</i> and <i>hasR</i> with their own promoters	This study

amplified by PCR using primers listed in Table S1 in the supplemental material.

The mini-CTX1 PpvdA'-mCherry construct was generated by cloning the mCherry coding sequence without the start codon into the integration-proficient plasmid mini-CTX1 (42) by HindIII/SalI digestion,

yielding mini-CTX1 mCherry (Table 1). The DNA fragment encompassing the *pvdA* promoter (from nucleotide -277 to nucleotide +10 relative to the start codon of *pvdA*) was then cloned into mini-CTX1 mCherry by EcoRI/HindIII digestion in order to generate mini-CTX1 PpvdA'-mCherry, harboring a translational fusion between the first three codons

of *pvdA* and the mCherry coding sequence, under the control of the *pvdA* promoter (Table 1). The mini-CTX *PpvdA'*-mCherry plasmid was conjugally transferred from *E. coli* S17-1 λ pir into *P. aeruginosa* strains to allow integration of the construct into the *attB* neutral site of the *P. aeruginosa* chromosome. Transconjugants were selected on tetracycline-containing LB agar plates.

Growth in the presence of human transferrin and in human serum.

Human serum samples (2.5 ml each) were collected from 130 healthy donors following submission, comprehension, and subscription of a written informed consent. Sera were pooled, filtered, and heat inactivated (30 min at 56°C) as previously described (43). Serum chemistry was as follows: total iron, 0.78 μ g/ml; ferritin, 0.21 μ g/ml; transferrin, 2.63 mg/ml; and total iron binding capacity, 3.16 μ g/ml (28% transferrin saturation, equivalent to 45.6 μ M unsaturated iron binding sites). To achieve complete transferrin saturation, an excess of FeCl_3 (100 μ M) was added to both DCAA-Tf and human serum. Bacterial strains were grown overnight at 37°C in DCAA, diluted to an optical density at 600 nm (OD_{600}) of 0.003 in DCAA-Tf or human serum, with or without FeCl_3 , and dispensed into 96-well microtiter plates. Growth (OD_{600}) was monitored periodically for up to 48 or 56 h in a Wallac 1420 Victor³ V multilabel plate reader (PerkinElmer).

Growth under microaerobic conditions. *P. aeruginosa* PAO1 and isogenic *feoB*, *tonB1 feoB*, and *tonB1* mutants containing the pMP220::P*feoA* plasmid (Table 1) were grown under low-oxygen conditions. Bacteria were inoculated into 12 ml of TSBD containing 1% KNO_3 (as a terminal electron acceptor) and 2 mM ascorbate (as a reducing agent), dispensed into 13-ml round-bottomed tubes (44), and topped with liquid paraffin, while the tube caps were sealed with Parafilm. TSBD was supplemented or not with FeSO_4 (2.5, 10, or 50 μ M) or with DIP (100 μ M). Cultures were incubated at 37°C under static conditions, and growth was measured by determining the OD_{600} after 24 h.

Growth in the presence of heme. The ability of the PAO1 wild type and the *hasR phuR* mutant to acquire heme was assessed as previously described (15), with minor modifications. Strains were grown for 16 h at 37°C in M9 medium containing 0.2% glucose and 100 μ M DIP. The cultures were diluted to ca. 10^5 to 10^6 cells ml^{-1} , and 100 μ l of each diluted culture was mixed with 4 ml M9 medium containing 0.2% glucose, 1 mM DIP, and 0.8% agarose (ultrapure agarose; Invitrogen) and poured onto plates of M9 medium containing 0.2% glucose, 1 mM DIP, and 1.5% agarose. Sterile filter disks were placed on top of the plates and spotted with 15 μ l of a 5-mg ml^{-1} stock solution of bovine hemin chloride (Sigma) in 10 mM NaOH or bovine hemoglobin (Sigma) in phosphate-buffered saline (PBS). The appearance of colonies around the filter disks was detected after 48 h of incubation at 37°C.

Siderophore assays. Pyoverdine production after 14 h of growth in DCAA (inoculum $\text{OD}_{600} \approx 0.001$) was measured in culture supernatants appropriately diluted in 100 mM Tris-HCl (pH 8) by absorbance readings at 405 nm normalized to the cell densities of the bacterial cultures (OD_{600}) (45). For pyoverdine purification, the *P. aeruginosa* PAO1 *pchD* mutant was grown in 30 ml of DCAA at 37°C for 24 h. Pyoverdine was purified from the culture supernatant by filtration through a Sep-Pack C_{18} Vac cartridge (3 ml; Waters). After solvation of the polymer packing with 10 hold-up volumes of 50% methanol, the cartridge was flushed with 10 hold-up volumes of double-distilled water. The filtered culture supernatant containing pyoverdine was loaded onto the column and washed several times with double-distilled water. The pigmented fluorescent material was then eluted with a small quantity of 50% (vol/vol) methanol, evaporated to dryness in a desiccator, and dissolved in 100 μ l of double-distilled water. The pyoverdine concentration was determined by spectrophotometric measurement of the apo form (OD_{405}) ($\epsilon = 1.4 \times 10^4 \text{ M}^{-1} \text{ cm}^{-1}$) (46).

For pyochelin measurement, the PAO1 wild type, the *pvdA*, *pchD*, and *pvdA pchD* mutant strains, and the complemented mutants were grown in GGP medium for 36 h. Pyochelin was partially purified by ethyl acetate extraction of acidified supernatants and resuspended in methanol, and

extracts (2.5 or 5 μ l) were separated by thin-layer chromatography (TLC) (silica gel 60F254; Merck), using acetone:methanol:0.2 M acetic acid (5:2:1) as the development solvent (47). Pyochelin spots on TLC plates were detected by yellow-green fluorescence emission under UV light or upon development by spraying with FeCl_3 , as described previously (36). Quantitative determination of pyochelin levels was performed by scraping the fluorescent spots from TLC plates and extracting them twice with methanol. The amount of apo-pyochelin in methanol extracts was determined by spectrophotometric measurement (OD_{330}) ($\epsilon = 4.4 \times 10^3 \text{ M}^{-1} \text{ cm}^{-1}$) (48).

Western blot analysis of ToxA expression and PrpL and β -galactosidase activity assays. For ToxA detection, cell-free culture supernatants were supplemented with 6 \times SDS-PAGE loading dye (375 mM Tris-HCl [pH 6.8], 9% SDS, 50% glycerol, 0.03% bromophenol blue). The volumes of supernatants (or appropriate dilutions) loaded in SDS-PAGE gels were normalized to bacterial growth according to the following formula: loading volume (microliters) = $10/\text{OD}_{600}$ for the corresponding bacterial culture (49). Proteins resolved by SDS-PAGE were electrotransferred to a nitrocellulose filter (Hybond-C Extra; Amersham) and probed for ToxA by using a rabbit polyclonal anti-ToxA antibody (Sigma-Aldrich). Filters were developed with ECL Prime (Amersham) and visualized on a Chemi-Doc XRS+ system (Bio-Rad). Densitometric analysis of band intensities was performed using Image Lab 3.0 software (Bio-Rad).

PrpL enzymatic activity was determined for 50- μ l aliquots of cell-free culture supernatants as previously described (50), using the chromogenic substrate Chromozym PL (tosyl-Gly-Pro-Lys-*p*-nitroanilide; Sigma-Aldrich), which is specific for PrpL (protease IV) and is not cleaved by other *P. aeruginosa* proteases (51).

β -Galactosidase activity from *P. aeruginosa* cells carrying the pMP220::P*feoA*, pPZ-*toxA*, or pPZ-*prpL* reporter plasmid (Table 1) was determined spectrophotometrically by using *o*-nitrophenyl- β -D-galactopyranoside as the substrate, normalized to the OD_{600} of the bacterial culture, and expressed in Miller units (M.U.) (52).

Mouse model of lung infection. To probe the iron availability in the mouse lung, the fluorescent *P. aeruginosa* reporter strains PAO1 *PpvdA'*-mCherry and PAO1 *pvdA pchD PpvdA'*-mCherry were grown for 16 h in DCAA and then diluted to ca. 6×10^7 and 6×10^8 CFU/ml, respectively, in sterile PBS supplemented or not with 10 μ M FeSO_4 . Four groups of four CD1 male mice (Charles River) were infected intranasally with 80 μ l of bacterial suspension (2 inocula of 20 μ l per nostril) supplemented or not with FeSO_4 . Two mice per group were sacrificed after 5 h, and the other two 24 h after infection, and bronchoalveolar lavages (BALs) were performed immediately to recover bacteria from the lungs. The presence of bacterium-associated mCherry fluorescence in BAL fluid samples was investigated by confocal microscopy (Leica SP5 confocal laser scanning microscope; 63 \times oil immersion objective) at an excitation wavelength of 585 nm.

To investigate the contributions of individual iron uptake systems to *P. aeruginosa* lung infectivity, the PAO1 wild type and isogenic single or double mutants in iron uptake systems were grown for 16 h in TSBD supplemented with 5 μ M FeSO_4 to support growth of the *tonB1* and *tonB1 feoB* mutants and then were transferred to fresh medium and grown for 4 to 5 h, to the mid-log phase. The cultures were centrifuged at $4,000 \times g$ for 15 min, and the cell pellets were washed twice with PBS and suspended in the original volume of liquid. The optical density was adjusted to obtain the desired inocula, and *P. aeruginosa* agar beads were prepared following an established method (33), using TSBD agar. C57BL/6 male mice (Charles River) were infected intratracheally with ca. 10^6 cells of each *P. aeruginosa* strain embedded in agar beads as described previously (33), and mortality was monitored for up to 14 days.

Animals were handled in compliance with European Communities Council Directive 86/609 for the care of laboratory animals and ethical guidelines for research in animals. Procedures were approved by the Institutional Animal Care and Use Committee (IACUC) of the San Raffaele Scientific Institute (Milan, Italy) and the Department of Food Safety and

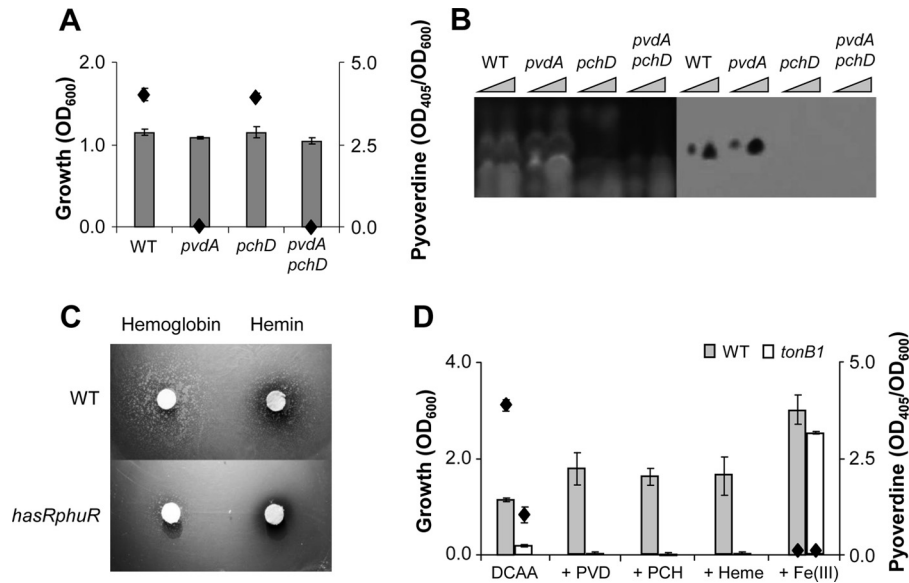


FIG 1 Iron uptake phenotypes of different *P. aeruginosa* iron uptake mutants. (A) Growth (bars; left y axis) and pyoverdine production (diamonds; right y axis) of the wild-type (WT) strain and the *pvdA*, *pchD*, and *pvdA pchD* mutants measured after 14 h of growth in the iron-poor medium DCAA. (B) Pyochelin extracted from culture supernatants of the WT, *pvdA*, *pchD*, and *pvdA pchD* strains after 36 h of growth in GGP medium and separated (2.5 or 5.0 μ l of extract) by thin-layer chromatography (TLC). Chromatograms were visualized by exposure to UV light (left) and by spraying with 100 μ M FeCl₃ (right). (C) Growth of the WT and *hasR phuR* strains in the presence of hemoglobin (left) or hemin (right) on M9 agarose plates containing 0.2% glucose and 1 mM DIP. (D) Growth (bars; left y axis) of the WT and *tonB1* strains at 24 h postinoculation in DCAA supplemented or not with pyoverdine (PVD; 20 μ M), pyochelin (PCH; 20 μ M), heme (heme; 20 μ M), or FeCl₃ [Fe(III); 50 μ M]. Pyoverdine production (diamonds; right y axis) was measured in the control medium (DCAA) and in DCAA supplemented with FeCl₃ [+Fe(III)]. Values in panels A and D are the means for three independent experiments \pm standard deviations (SD). Pictures in panels B and C are representative of three independent experiments giving similar results.

Veterinary Public Health, Istituto Superiore di Sanità (Rome, Italy), and adhered strictly to the Italian Ministry of Health guidelines for the use and care of experimental animals.

Statistical analysis. Statistical analysis was performed with GraphPad Prism software, using one-way analysis of variance (ANOVA) (for growth yield analysis) and the log rank Mantel-Cox test (for survival curve analysis). A first-type error probability of 0.05 was considered significant.

RESULTS

In vitro phenotypes of iron uptake mutants. To gain insight into the role of iron in *P. aeruginosa* virulence, a set of mutants impaired in single or multiple iron uptake systems was generated in the reference strain PAO1, and their phenotypes were tested. The siderophore mutants, i.e., the pyoverdine mutant (*pvdA*), the pyochelin mutant (*pchD*), and the siderophore-null double mutant (*pvdA pchD*), were verified to lack pyoverdine and/or pyochelin production in the iron-poor media DCAA and GGP (Fig. 1A and B). The heme uptake mutant (*hasR phuR*) was verified to have growth impairment in the presence of heme as the sole iron source (Fig. 1C). The growth of all these mutants was either unaffected or moderately reduced in DCAA (Fig. 1; not shown for the *hasR phuR* mutant). Conversely, growth of the Fe(III) uptake mutant (*tonB1*) was impaired in DCAA unless the medium was supplemented with an excess of iron (Fig. 1D). Addition of pyoverdine, pyochelin, or heme did not restore the growth of the *tonB1* mutant, while it slightly stimulated the growth of the wild type (Fig. 1D), consistent with the essential role of the TonB system in siderophore and heme/hemophore translocation across the outer membrane (16, 17). For all deletion mutants, the iron uptake-defective phenotypes were rescued when a copy of the deleted

gene(s) with the indigenous promoter was provided in *trans* on plasmid pUCP18 (see Fig. S1 in the supplemental material).

The *feoB* and *tonB1 feoB* Fe(II) uptake mutants were compared with the corresponding parental strains (PAO1 and the *tonB1* mutant, respectively) for the ability to grow in the iron-depleted medium TSBD containing 1% KNO₃ and 2 mM ascorbate under both aerobic and microaerobic conditions (Fig. 2). To allow mi-

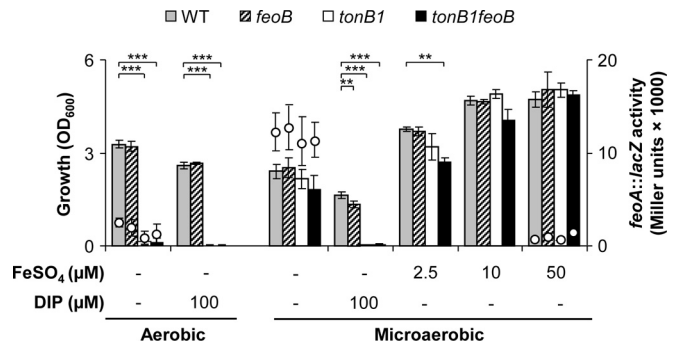


FIG 2 Role of the Feo system under aerobic and microaerobic growth conditions. The graph shows the growth (bars; left y axis) and activity of the *feoA::lacZ* iron-regulated fusion (circles; right y axis) of the wild type (WT) and the *feoB*, *tonB1*, and *tonB1 feoB* mutants after 24 h of growth under aerobic and microaerobic conditions in TSBD (supplemented with 1% KNO₃ for microaerobic growth). Data are the means \pm SD for six independent experiments. Statistical analysis (ANOVA followed by Tukey's multiple-comparison test) was performed on bacterial growth results, and statistically significant differences with respect to the WT are indicated as follows: **, $P < 0.01$; ***, $P < 0.001$.

croaerobic growth of *P. aeruginosa* in TSBD, the terminal electron acceptor KNO_3 appeared to be essential (53, 54; data not shown). Under aerobic conditions, growth of the *tonB1* and *tonB1 feoB* mutants was severely impaired in TSBD and was further inhibited by the presence of the Fe(II) chelator DIP (Fig. 2), consistent with our previous observations in DCAA (Fig. 1D). Under microaerobic conditions in the presence of the reducing agent ascorbate, where Fe(II) is expected to represent the prevalent form of iron, both the *tonB1* and *tonB1 feoB* mutants grew well, attaining nearly the same levels as the corresponding parental strains (Fig. 2). Unexpectedly, growth of the *feoB* and *tonB1 feoB* Fe(II) uptake mutants was not significantly different from that observed for wild-type PAO1 and the *tonB1* mutant, respectively (Fig. 2). A transcriptional fusion between *lacZ* and the promoter of the *feo* operon (*PfeoA*), which is expected to be active under low-iron and low-oxygen conditions (23, 55), was highly expressed by all the tested strains, confirming that iron was limiting during microaerobic growth (Fig. 2).

Under microaerobic conditions, the addition of DIP (100 μM) slightly reduced the growth of the *feoB* mutant with respect to that of PAO1, while the growth of the *tonB1* and *tonB1 feoB* strains was completely inhibited (Fig. 2). Addition of increasing concentrations of Fe(II) (2.5 to 50 μM FeSO_4) stimulated the growth of all strains, although to a lesser extent for the *tonB1 feoB* mutant. As expected, expression of the iron-regulated *PfeoA::lacZ* transcriptional fusion was completely shut down at 50 μM FeSO_4 (Fig. 2). Taken together, these results suggest the existence in *P. aeruginosa* of an alternative route(s) for the acquisition of Fe(II) that enables the *feoB* mutant to grow under microaerobic conditions in Fe(II)-poor environments.

Efficacy of iron uptake systems in competing for iron with human transferrin. To investigate the capability of *P. aeruginosa* iron uptake systems to compete for iron with human transferrin, wild-type PAO1 and the iron uptake mutants were tested for the ability to grow in DCAA supplemented with human transferrin (DCAA-Tf) at 2.5 mg/ml (approximately the transferrin concentration in human serum) (see Materials and Methods for details). The *feoB*, *pchD*, and *hasR phuR* mutant strains grew as well as the PAO1 wild type in DCAA-Tf, while growth of both the *pvdA* and *pvdA pchD* mutants was strongly reduced (Fig. 3A). Remarkably, growth of both the *tonB1* and *tonB1 feoB* mutants was completely inhibited (Fig. 3A), suggesting that Fe(III) uptake systems are essential in the competition with transferrin and that pyoverdine plays the primary role. Addition of an excess of iron (100 μM FeCl_3) ensured the growth of all mutants at levels comparable to those of the wild type and much higher than those observed in DCAA-Tf without added iron (Fig. 3A).

Growth of all strains was also tested in heat-inactivated human serum, with or without 100 μM FeCl_3 (Fig. 3B). While growth of the *feoB*, *pchD*, and *hasR phuR* mutants was comparable to that of the wild type, neither the *pvdA* and *pvdA pchD* nor *tonB1* and *tonB1 feoB* mutants were able to grow in human serum unless exogenous iron was added (Fig. 3B). In agreement with previous findings (29, 56, 57), our data corroborate the crucial role of pyoverdine for *P. aeruginosa* growth in human serum and show that the other iron uptake systems are dispensable under these growth conditions.

Probing iron availability in the mouse lung during *P. aeruginosa* infection. Before testing the virulence of *P. aeruginosa* iron uptake mutants in a mouse model of experimental lung infection,

iron bioavailability in the mouse lung was assessed. For this purpose, a reporter system based on the *PvdS*-controlled *pvdA* promoter (58) fused to the gene for the fluorescent protein mCherry (Table 1) was introduced into the genomes of wild-type PAO1 and the *pvdA pchD* double mutant (Fig. 4; see Fig. S2 in the supplemental material). Detectable fluorescence was associated with the cells of both strains grown in DCAA and was absent upon growth in DCAA containing $\geq 10 \mu\text{M}$ FeSO_4 (Fig. 4; see Fig. S2). Mice were inoculated intranasally with 5×10^6 and 5×10^7 CFU of each of the fluorescent reporter strains grown in DCAA, and mCherry-related fluorescence was assessed in bacterial cells recovered from the BAL fluid of infected mice at 5 and 24 h postinfection. No mortality was observed during infection (data not shown). Both wild-type and *pvdA pchD* mutant cells carrying the *PpvdA'*-mCherry fusion appeared fluorescent when recovered from the BAL fluid at 5 and 24 h postinfection, while fluorescence was undetectable at any time when the bacterial inoculum was supplemented with iron (10 μM FeSO_4) (Fig. 4; see Fig. S2). Upon visual comparison, more fluorescence was associated with the *pvdA pchD* mutant than with wild-type PAO1 (Fig. 4; see Fig. S2), as expected for a siderophore-null mutant, which experiences more pronounced iron starvation, thus showing increased expression of the reporter system. Most importantly, these *in vivo* experiments demonstrate that *P. aeruginosa* perceives the mouse lung as an iron-poor environment at the onset of infection.

Contributions of individual iron uptake systems to *P. aeruginosa* lung infectivity. Wild-type PAO1 and all iron transport mutants were tested for pathogenicity by use of a well-established model of mouse pneumonia (31, 33). Mortality due to secondary septicemia was monitored for up to 14 days after the challenge.

Almost all mice infected with wild-type PAO1 died within 7 days postinfection (10% survival). The *feoB*, *hasR phuR*, and *pchD* mutant strains also caused relatively high mortality, with 20% to 45% mouse survival rates (Fig. 5), while both the *tonB1* and *tonB1 feoB* strains were completely avirulent in this infection model (Fig. 5). Notably, mice infected with *pvdA* and *pvdA pchD* strains displayed 77% and 85% survival rates, respectively (Fig. 5). These results signify that among *P. aeruginosa* iron uptake systems, pyoverdine has the most prominent role and is required for successful mouse lung infection.

Dual roles of pyoverdine in mouse lung infection. Interaction of ferripyoverdine with the FpvA receptor triggers a signal through the inner-membrane-spanning anti-sigma factor FpvR, leading to the activation of the alternative sigma factor PvdS (21, 26). As summarized in Fig. 6A, PvdS controls, either directly or indirectly, not only the pyoverdine synthesis genes but also the expression of key *P. aeruginosa* virulence genes, such as the *prpL* and *toxA* genes, encoding the PrpL endoprotease and exotoxin A, respectively (26). Therefore, pyoverdine serves both as an iron carrier *in vivo* and as an activating signal of *P. aeruginosa* virulence. Given these dual roles, an attempt was made to distinguish between the siderophore and virulence-inducing signal functions of pyoverdine *in vivo*. For this purpose, we generated a *pvdA fpvR* double mutant as well as an *fpvR* single mutant (as a control). In the *fpvR* mutants, PvdS activity is not repressed by the FpvR anti-sigma factor, and therefore PvdS-dependent virulence genes (*prpL* and *toxA*) are expressed irrespective of the activation state of the pyoverdine signaling cascade. In fact, the *pvdA* mutant was found to release lower levels of the PrpL and

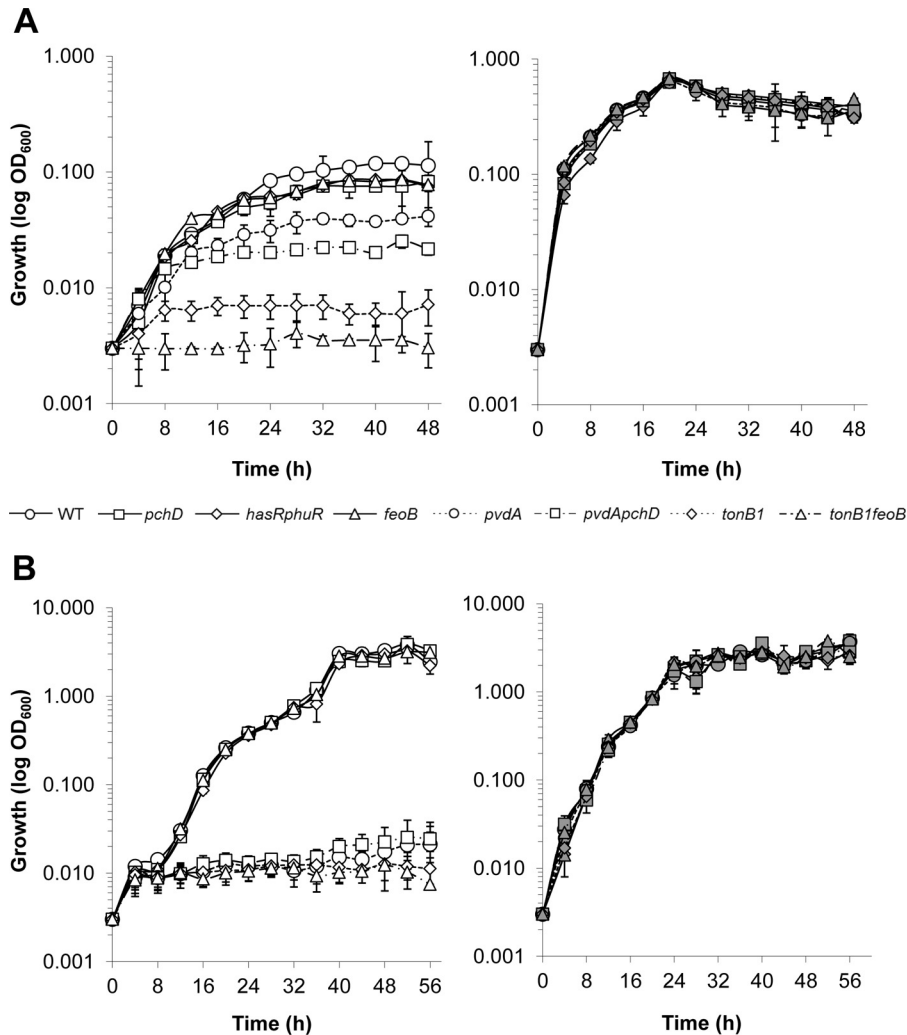


FIG 3 *P. aeruginosa* growth in the presence of human transferrin. The wild type (WT) and the iron uptake mutants were grown in DCAA supplemented with 2.5 mg/ml human transferrin (A) and in complement-free human serum (B) for up to 48 and 56 h, respectively, in the absence (left panels, white symbols) or presence (right panels, gray symbols) of 100 μ M FeCl₃. For each strain, the mean value \pm SD for three independent microtiter plate assays was considered.

ToxA virulence factors due to the lack of ferripyoverdine signaling via FpvA, while the introduction of the *fpvR* mutation in the *pvdA* background restored the *in vitro* production of PrpL and ToxA (Fig. 6B and C). The levels of the virulence factors in culture supernatants correlated well with the β -galactosidase activities expressed by reporter plasmids carrying the *PprpL* or *PtoxA* promoter (Fig. 6D).

In the mouse model of infection, the *pvdA* mutant was strongly impaired in virulence, resulting in nearly the same lethality as that of the *pvdS* mutant, which produces neither pyoverdine nor pyoverdine-induced virulence factors (25, 26, 59). Conversely, the *pvdA fpvR* mutant showed significantly increased virulence (about 60% lethality) compared to that of the *pvdA* mutant. Since the *pvdA fpvR* mutant was defective in pyoverdine-mediated iron uptake, its increased pathogenicity compared to that of the *pvdA* mutant could be ascribed to the restored production of PvdS-dependent virulence factors due to the *fpvR* mutation (Fig. 6E). This observation provides the first direct evidence that pyoverdine contributes to the pathogenesis of *P. aeruginosa*

lung infection by combining iron transport and virulence-inducing capabilities.

DISCUSSION

Iron is an essential nutrient for bacterial pathogens. To cope with the iron limitation that characterizes healthy host tissues, pathogenic bacteria must actively acquire iron through high-affinity transport mechanisms. Accordingly, numerous data providing evidence of the role of iron uptake in bacterial pathogenicity were provided over years (reviewed in references 6 and 60). The majority of bacterial pathogens are genetically determined to acquire iron from several iron sources, including endogenous and exogenous siderophores, heme or heme-binding proteins, and the soluble Fe²⁺ ion. However, the hierarchy according to which individual iron uptake systems contribute to *in vivo* virulence is not always clear.

Here we used a mouse model of pulmonary infection to assess the roles of different iron acquisition systems in lung pathogenicity by *P. aeruginosa*, which represents a typical example of an op-

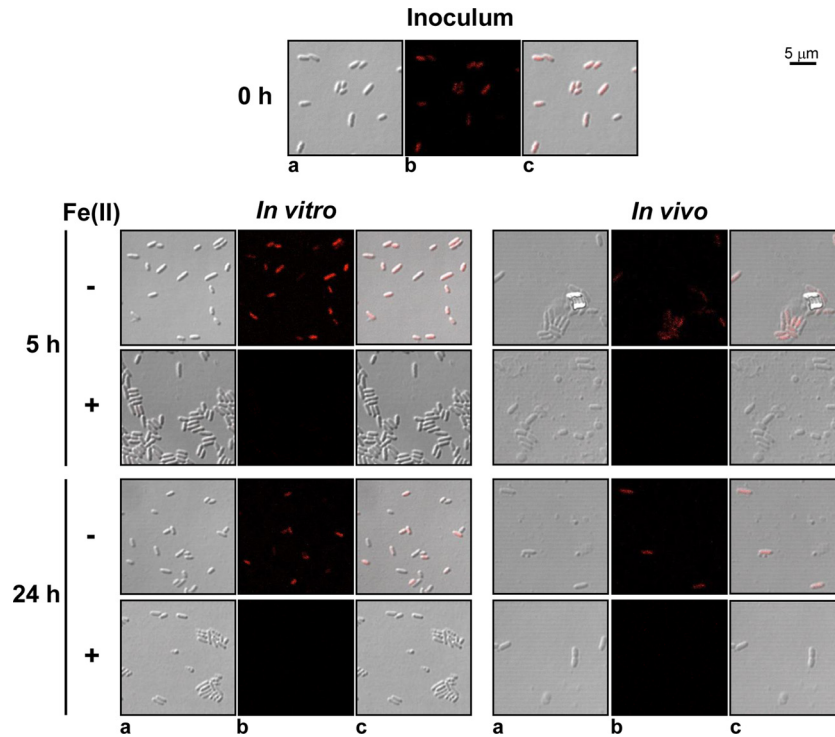


FIG 4 The *pvdA pchD* mutant perceives the mouse lung as an iron-poor environment. Confocal microscopy images showing the *in vitro* and *in vivo* fluorescence of the *pvdA pchD* mutant carrying the *PpvdA'*-mCherry fusion. Bacterial cultures were grown in the iron-poor medium DCAA, observed by confocal microscopy (0 h), and diluted to obtain 6×10^8 CFU/ml. For the *in vitro* experiment, bacteria were grown in DCAA supplemented or not with $10 \mu\text{M}$ FeSO_4 , and samples were analyzed after 5 h and 24 h. For the *in vivo* experiment, mice were inoculated with a bacterial suspension in PBS supplemented or not with $10 \mu\text{M}$ FeSO_4 . After 5 h and 24 h of infection, BALs were performed, and BAL fluid was analyzed by confocal microscopy. Panels show pictures taken under visible light with differential interference contrast (DIC) (a), the fluorescence emission upon excitation at 585 nm (b), and the overlay of visible and fluorescence images (c). Representative images are shown. A Leica SP5 confocal laser scanning microscope equipped with a $63\times$ oil immersion objective was used.

opportunistic pathogen endowed with broad iron uptake capabilities (7, 8). By generating and testing single and double deletion mutants in all the iron uptake systems described so far, we confirmed that Fe^{3+} acquisition is essential for *P. aeruginosa* infectivity in the mouse pneumonia model, as testified by the avirulent phenotype of mutants lacking the TonB energy transduction system for Fe^{3+} transport across the outer membrane (Fig. 5). Among Fe^{3+} sources, endogenous siderophores appear to be more important than heme, since mice infected with the heme uptake-defective *hasR phuR* double mutant showed lethality nearly comparable to that with the wild type and opposite to that with the pyoverdine- and pyochelin-deficient double mutant, which showed an avirulent behavior resembling that of the *tonB1* mutant(s) (Fig. 5). Impaired pyoverdine production had a stronger impact than pyochelin deficiency on *P. aeruginosa* lung pathogenicity (Fig. 5). This effect cannot be ascribed exclusively to more favorable iron-binding properties of pyoverdine than of pyochelin but also to the crucial role of pyoverdine as a virulence-activating signal molecule (21, 26). The generation of a pyoverdine-deficient strain in which the expression of the virulence factors PrpL and ToxA is independent of pyoverdine signaling (*pvdA fpvR*) made it possible to demonstrate that pyoverdine actually contributes to pathogenicity in the mouse lung infection model through iron uptake and virulence induction activities (Fig. 6). Interestingly, the lethality observed for the *pchD* (pyochelin) and *pvdA fpvR* (pyoverdine) mutants were nearly comparable (ca. 50%), suggesting that both pyochelin and pyoverdine provide important contributions to

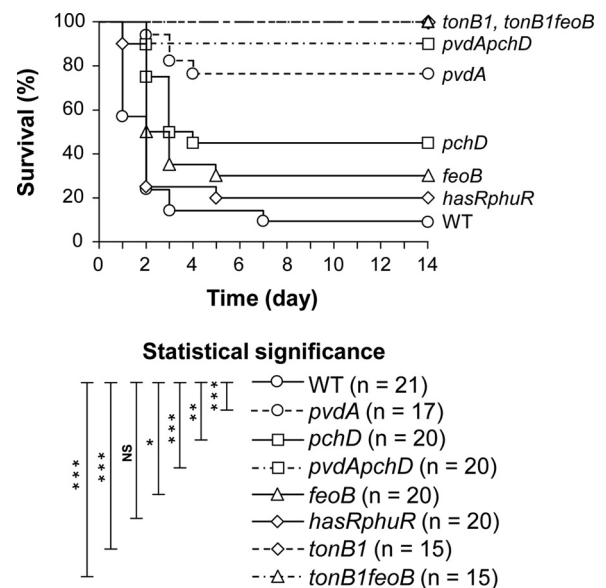


FIG 5 Iron uptake and *P. aeruginosa* virulence in a mouse model of pulmonary infection. Mice were infected intratracheally with 2×10^6 *P. aeruginosa* cells of wild-type (WT) PAO1 or of each iron uptake mutant embedded in agar beads. Mortality was monitored for 14 days after challenge. Data were pooled from two independent experiments (values for *n* indicate total numbers of mice). The statistical significance of differences in survival curves with respect to the WT are indicated as follows (Mantel-Cox test): *, $P < 0.05$; **, $P < 0.01$; ***, $P < 0.001$; and NS, not statistically significant.

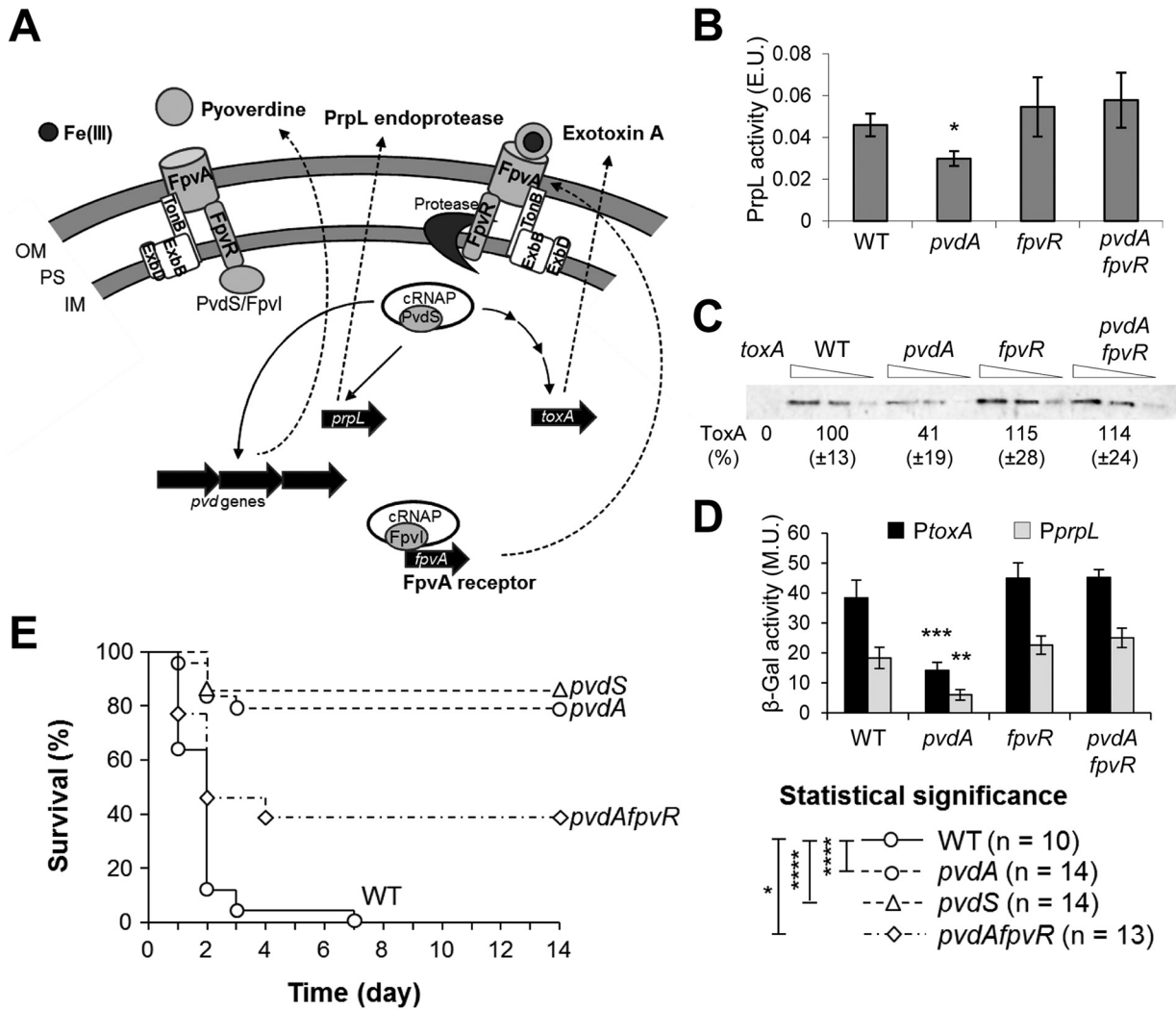


FIG 6 Pyoverdine signaling and *P. aeruginosa* lung pathogenicity. (A) Schematic of pyoverdine signaling. (Left) In the absence of ferripyoverdine, the TonB-dependent FpvA receptor cannot transmit a signal to the membrane-spanning anti-sigma factor FpvR, which retains the sigma factors PvdS and FpvI in an inactive state. (Right) Binding of ferripyoverdine determines a conformational change in the FpvA receptor that triggers FpvR proteolysis and release of the PvdS and FpvI sigma factors, which can bind the core RNA polymerase (cRNAP) and initiate transcription. PvdS-dependent RNAP directs the transcription of pyoverdine synthesis genes, the endoprotease PrpL gene (*prpL*), and, indirectly, the exotoxin A gene (*toxA*). FpvI-dependent RNAP transcribes the receptor FpvA gene (*fpvA*). In the absence of the anti-sigma factor FpvR (i.e., in the *pvdA fpvR* mutant strain), PvdS is predicted to be constitutively active. Multiple arrows on the pathway denote a multistep regulation. (B and C) PrpL enzymatic units (E.U.) (B) and exotoxin A levels (expressed as percentages relative to the level in PAO1) (C) in supernatants from wild-type PAO1 (WT), *pvdA*, *fpvR*, and *pvdA fpvR* cultures grown for 16 h in TSBD. For Western blot analysis, the undiluted supernatant and two 1:2 serial dilutions were loaded into the gels for each strain, while the undiluted supernatant from a *toxA* mutant was used as a negative control. (D) β -Galactosidase activities in WT, *pvdA*, *fpvR*, and *pvdA fpvR* cells carrying the pPZ-*toxA* (black bars) or pPZ-*prpL* (gray bars) promoter-probe plasmid after 16 h of growth in TSBD. Values in panels B to D represent the means \pm SD for at least three independent experiments. Asterisks denote statistically significant differences relative to the WT (*, $P < 0.05$; **, $P < 0.01$; ***, $P < 0.001$) (ANOVA). (E) Virulence of the WT, *pvdA*, *pvdA fpvR*, and *pvdS* strains in the mouse model of pulmonary infection. Data were pooled from two independent experiments (values for *n* indicate the total numbers of mice). The statistical significance of differences in survival curves with respect to the WT are indicated as follows (Mantel-Cox test): *, $P < 0.05$; and ****, $P < 0.0001$.

siderophore-mediated iron uptake in the lung (Fig. 5 and 6). This is an intriguing result considering the significantly lower affinity for iron of pyochelin than that of pyoverdine, at least *in vitro* (9, 10, 12, 13). Since it has been demonstrated that pyoverdine has a primary role in withdrawing iron from transferrin and lactoferrin (61, 62) and is essential for *P. aeruginosa* growth in human serum (Fig. 3) (56, 57), as well as for pathogenicity in a mouse model of systemic infection (29), our data suggest that specific features of the lung environment somehow foster the iron-chelating activity of pyochelin during pulmonary infection. Notably, expression of

pyochelin genes was recently documented for *P. aeruginosa* cells infecting the lungs of CF patients (55), and pyochelin production was found to be induced in a CF epidemic strain in artificial CF sputum medium (63).

Note that the mouse model used in this study, established by PAO1 infection, was characterized by severe pneumonia (Fig. 5 and 6) (31) and multiorgan dissemination of bacterial cells (with *P. aeruginosa* counts of $>10^3$ in spleens of moribund mice [data not shown]), which led to fulminant sepsis and a high mortality rate (80 to 90%). These conditions resemble those of acute *P.*

aeruginosa pneumonia in humans, which is associated with high mortality and can eventually degenerate into septicemia (1, 2). This pathological situation differs greatly from chronic lung infections established by *P. aeruginosa* in CF patients, which can partly be mimicked in mice by using pathoadaptive CF isolates capable of persisting in the lungs without causing death (34). Indeed, the constitutive inflammatory state which characterizes the airways of CF patients as a result of chronic bacterial infections (64) makes CF lungs a completely different environment from the lungs of healthy individuals. While iron is barely detectable in normal airway secretions, sputa from chronically infected CF patients contain micromolar concentrations of iron (65, 66). This increase in total iron probably derives from tissue damage due to the combined actions of inflammation and infection, as well as by defective iron trafficking by CF epithelial cells (67). Thus, the interplay between the host and the infecting pathogen(s) changes the lung pathophysiology in CF patients, and this likely results in the availability of iron sources which are unavailable in healthy lungs. This is indirectly corroborated by the observation that while pyoverdine is essential for establishing infection in our mouse model of acute pneumonia (Fig. 5 and 6), pyoverdine-deficient isolates accumulate over the course of chronic infection in CF patients (68–70). Although many of these isolates can still behave as siderophore cheaters, exploiting the supply of pyoverdine provided by cooperative producers in mixed *P. aeruginosa* populations (70), recent evidence strongly suggests that other iron acquisition strategies can be employed by *P. aeruginosa* to persist in the chronically infected CF lung. Notably, it has been found that the soluble Fe^{2+} ion represents the main iron source in late-stage CF disease (71), when oxygen tension in the lung is very low and *P. aeruginosa* grows mainly as dense, biofilm-like microcolonies in locally anoxic microenvironments (72). Conversely, the master regulator of the pyoverdine system, PvdS, was previously shown to be required for infection of tissues preferentially exposed to high O_2 tensions (30). Thus, although the *feoB* mutant displayed a slightly reduced ability to cause infection compared to the wild-type strain in our animal model (Fig. 5), the role of Feo in iron acquisition may become more relevant during chronic CF infection or under any other condition where O_2 tensions are low and Fe^{2+} represents the main iron species. Accordingly, a recent real-time PCR analysis detected *feoB* mRNA in the sputa of all CF patients analyzed (55). Intriguingly, our *in vitro* results showed that *P. aeruginosa feoB* and *tonB1* deletion mutants retained the ability to grow under anaerobic conditions when Fe^{2+} represented the prevalent form of iron (Fig. 2), strongly suggesting that an alternative (Feo-independent) mechanism for Fe^{2+} internalization exists in *P. aeruginosa*. Fe^{2+} uptake systems different from Feo have been described for other bacteria, such as the EfeUOB and FetMP systems of *E. coli* or the FtrABCD system of *Bordetella pertussis*, all belonging to the same protein family as the *Saccharomyces cerevisiae* Ftr1 iron transporter (73–75). Bioinformatic searches for homologs of the inner membrane transporters EfeU, FetM, and FtrC revealed the presence of a gene (PA5248) in the *P. aeruginosa* PAO1 genome encoding a putative Ftr1-like Fe^{2+} / Pb^{2+} permease, which is present in all *Pseudomonas* species sequenced so far, with the exception of *P. fulva* and *P. stutzeri* (www.pseudomonas.com). Whether PA5248 accounts for the retained ability of a *P. aeruginosa feoB* mutant under low-oxygen reducing conditions remains to be established. Very recently, a novel putative siderophore system which plays important roles in *P. aeruginosa* viability *in vitro* in

airway mucus secretions and in infectivity in burn wound and airway infection mouse models was identified (76), supporting the hypothesis that still unexplored iron uptake functions may be encoded by the *P. aeruginosa* genome.

Besides Fe^{2+} , two independent studies recently observed that reduction of pyoverdine production in different *P. aeruginosa* isolates from late chronic CF infections is accompanied by a more efficient utilization of heme as an iron source, suggesting that *P. aeruginosa* can evolve toward heme acquisition during CF lung colonization, plausibly as a consequence of increased availability of hemoglobin (77, 78). Finally, it should be noted that both experimental evidence and bioinformatic predictions revealed that *P. aeruginosa* has an impressive capability to acquire iron from several xenosiderophores (reviewed in reference 21). Thus, it cannot be excluded that in polymicrobial communities, such as those transiently occurring in the lungs of CF patients (79), other exogenous iron chelators may contribute to *P. aeruginosa* persistence and pathogenicity.

In conclusion, this work provides evidence that iron acquisition during acute *P. aeruginosa* lung infection is multifactorial, with individual iron uptake mechanisms contributing to different extents to the success of the pathogenic process. Moreover, the essential role of TonB-mediated iron uptake in the establishment of lung infection and the prominent contribution of the pyoverdine siderophore to *in vivo* virulence further support the recent efforts directed toward targeting iron metabolism and/or pyoverdine to exploit alternative therapeutic strategies for the treatment of *P. aeruginosa* infections (31, 80, 81).

ACKNOWLEDGMENTS

We are grateful to Camilla Riva and Ida De Fino for assistance with experimental infections.

This work was supported by grants from the Italian Cystic Fibrosis Foundation (grant FFC14/2010) and the Italian Ministry of University and Research (PRIN 2012; grant 2012WJSX8K) to P.V.

REFERENCES

- Fujitani S, Sun HY, Yu VL, Weingarten JA. 2011. Pneumonia due to *Pseudomonas aeruginosa*. Part I. Epidemiology, clinical diagnosis, and source. *Chest* 139:909–919. <http://dx.doi.org/10.1378/chest.10-0166>.
- Kollef MH, Chastre J, Fagon JY, François B, Niederman MS, Rello J, Torres A, Vincent JL, Wunderink RG, Go KW, Rehm C. 2014. Global prospective epidemiologic and surveillance study of ventilator-associated pneumonia due to *Pseudomonas aeruginosa*. *Crit Care Med* 42:2178–2187. <http://dx.doi.org/10.1097/CCM.0000000000000510>.
- Döring G, Parameswaran IG, Murphy TF. 2011. Differential adaptation of microbial pathogens to airways of patients with cystic fibrosis and chronic obstructive pulmonary disease. *FEMS Microbiol Rev* 35:124–146. <http://dx.doi.org/10.1111/j.1574-6976.2010.00237.x>.
- Folkesson A, Jelsbak L, Yang L, Johansen HK, Ciofu O, Høiby N, Molin S. 2012. Adaptation of *Pseudomonas aeruginosa* to the cystic fibrosis airway: an evolutionary perspective. *Nat Rev Microbiol* 10:841–851. <http://dx.doi.org/10.1038/nrmicro2907>.
- Ciofu O, Hansen CR, Høiby N. 2013. Respiratory bacterial infections in cystic fibrosis. *Curr Opin Pulm Med* 19:251–258. <http://dx.doi.org/10.1097/MCP.0b013e32835f1afc>.
- Nairz M, Schroll A, Sonnweber T, Weiss G. 2010. The struggle for iron—a metal at the host-pathogen interface. *Cell Microbiol* 12:1691–1702. <http://dx.doi.org/10.1111/j.1462-5822.2010.01529.x>.
- Cornelis P, Dingemans J. 2013. *Pseudomonas aeruginosa* adapts its iron uptake strategies in function of the type of infections. *Front Cell Infect Microbiol* 3:75. <http://dx.doi.org/10.3389/fcimb.2013.00075>.
- Poole K, McKay GA. 2003. Iron acquisition and its control in *Pseudomonas aeruginosa*: many roads lead to Rome. *Front Biosci* 8:d661–d686. <http://dx.doi.org/10.2741/1051>.

9. Wendenbaum S, Demange P, Dell A, Meyer JM, Abdallah MA. 1983. The structure of pyoverdine Pa, the siderophore of *Pseudomonas aeruginosa*. *Tetrahedron Lett* 24:4877–4880. [http://dx.doi.org/10.1016/S0040-4039\(00\)94031-0](http://dx.doi.org/10.1016/S0040-4039(00)94031-0).
10. Briskot G, Taraz K, Budzikiewicz H. 1989. Pyoverdine-type siderophores from *Pseudomonas aeruginosa*. *Liebigs Ann Chem* 1989:375–384. <http://dx.doi.org/10.1002/jlac.198919890164>.
11. Visca P, Imperi F, Lamont IL. 2007. Pyoverdine siderophores: from biogenesis to biosignificance. *Trends Microbiol* 15:22–30. <http://dx.doi.org/10.1016/j.tim.2006.11.004>.
12. Cox CD, Graham R. 1979. Isolation of an iron-binding compound from *Pseudomonas aeruginosa*. *J Bacteriol* 137:357–364.
13. Brandel J, Humbert N, Elhabiri M, Schalk IJ, Mislin GL, Albrecht-Gary AM. 2012. Pyochelin, a siderophore of *Pseudomonas aeruginosa*: physicochemical characterization of the iron(III), copper(II) and zinc(II) complexes. *Dalton Trans* 41:2820–2834. <http://dx.doi.org/10.1039/c1dt11804h>.
14. Schalk IJ, Guillon L. 2013. Fate of ferrisiderophores after import across bacterial outer membranes: different iron release strategies are observed in the cytoplasm or periplasm depending on the siderophore pathways. *Amino Acids* 44:1267–1277. <http://dx.doi.org/10.1007/s00726-013-1468-2>.
15. Ochsner UA, Johnson Z, Vasil ML. 2000. Genetics and regulation of two distinct haem-uptake systems, phu and has, in *Pseudomonas aeruginosa*. *Microbiology* 146:185–198. <http://dx.doi.org/10.1099/00221287-146-1-185>.
16. Noinaj N, Guillier M, Barnard TJ, Buchanan SK. 2010. TonB-dependent transporters: regulation, structure, and function. *Annu Rev Microbiol* 64:43–60. <http://dx.doi.org/10.1146/annurev.micro.112408.134247>.
17. Takase H, Nitani H, Hoshino K, Otani T. 2000. Requirement of the *Pseudomonas aeruginosa* tonB gene for high-affinity iron acquisition and infection. *Infect Immun* 68:4498–4504. <http://dx.doi.org/10.1128/IAI.68.8.4498-4504.2000>.
18. Zhao Q, Poole K. 2000. A second tonB gene in *Pseudomonas aeruginosa* is linked to the *exbB* and *exbD* genes. *FEMS Microbiol Lett* 184:127–132. <http://dx.doi.org/10.1111/j.1574-6968.2000.tb09002.x>.
19. Huang B, Ru K, Yuan Z, Whitchurch CB, Mattick JS. 2004. tonB3 is required for normal twitching motility and extracellular assembly of type IV pili. *J Bacteriol* 186:4387–4389. <http://dx.doi.org/10.1128/JB.186.13.4387-4389.2004>.
20. Cornelis P, Matthijs S. 2002. Diversity of siderophore-mediated iron uptake systems in fluorescent pseudomonads: not only pyoverdines. *Environ Microbiol* 4:787–798. <http://dx.doi.org/10.1046/j.1462-2920.2002.00369.x>.
21. Llamas MA, Imperi F, Visca P, Lamont IL. 2014. Cell-surface signaling in *Pseudomonas*: stress responses, iron transport, and pathogenicity. *FEMS Microbiol Rev* 38:569–597. <http://dx.doi.org/10.1111/1574-6976.12078>.
22. Cartron ML, Maddocks S, Gillingham P, Craven CJ, Andrews SC. 2006. Feo-transport of ferrous iron into bacteria. *Biometals* 19:143–157. <http://dx.doi.org/10.1007/s10534-006-0003-2>.
23. Ochsner UA, Wilderman PJ, Vasil AI, Vasil ML. 2002. GeneChip expression analysis of the iron starvation response in *Pseudomonas aeruginosa*: identification of novel pyoverdine biosynthesis genes. *Mol Microbiol* 45:1277–1287. <http://dx.doi.org/10.1046/j.1365-2958.2002.03084.x>.
24. Cornelis P, Matthijs S, Van Oeffelen L. 2009. Iron uptake regulation in *Pseudomonas aeruginosa*. *Biometals* 22:15–22. <http://dx.doi.org/10.1007/s10534-008-9193-0>.
25. Wilderman PJ, Vasil AI, Johnson Z, Wilson MJ, Cunliffe HE, Lamont IL, Vasil ML. 2001. Characterization of an endoprotease (PrpL) encoded by a PvdS-regulated gene in *Pseudomonas aeruginosa*. *Infect Immun* 69:5385–5394. <http://dx.doi.org/10.1128/IAI.69.9.5385-5394.2001>.
26. Lamont IL, Beare PA, Ochsner U, Vasil AI, Vasil ML. 2002. Siderophore-mediated signaling regulates virulence factor production in *Pseudomonas aeruginosa*. *Proc Natl Acad Sci U S A* 99:7072–7077. <http://dx.doi.org/10.1073/pnas.092016999>.
27. Bullen JJ, Ward CG, Wallis SN. 1974. Virulence and the role of iron in *Pseudomonas aeruginosa* infection. *Infect Immun* 10:443–450.
28. Cox CD. 1982. Effect of pyochelin on the virulence of *Pseudomonas aeruginosa*. *Infect Immun* 36:17–23.
29. Meyer JM, Neely A, Stintzi A, Georges C, Holder IA. 1996. Pyoverdine is essential for virulence of *Pseudomonas aeruginosa*. *Infect Immun* 64:518–523.
30. Xiong YQ, Vasil ML, Johnson Z, Ochsner UA, Bayer AS. 2000. The oxygen- and iron-dependent sigma factor *pvdS* of *Pseudomonas aeruginosa* is an important virulence factor in experimental infective endocarditis. *J Infect Dis* 181:1020–1026. <http://dx.doi.org/10.1086/315338>.
31. Imperi F, Massai F, Facchini M, Frangipani E, Visaggio D, Leoni L, Bragonzi A, Visca P. 2013. Repurposing the antimycotic drug flucytosine for suppression of *Pseudomonas aeruginosa* pathogenicity. *Proc Natl Acad Sci U S A* 110:7458–7463. <http://dx.doi.org/10.1073/pnas.1222706110>.
32. Takase H, Nitani H, Hoshino K, Otani T. 2000. Impact of siderophore production on *Pseudomonas aeruginosa* infections in immunosuppressed mice. *Infect Immun* 68:1834–1839. <http://dx.doi.org/10.1128/IAI.68.4.1834-1839.2000>.
33. Bragonzi A, Paroni M, Nonis A, Cramer N, Montanari S, Rejman J, Di Serio C, Döring G, Tümmler B. 2009. *Pseudomonas aeruginosa* microevolution during cystic fibrosis lung infection establishes clones with adapted virulence. *Am J Respir Crit Care Med* 180:138–145. <http://dx.doi.org/10.1164/rccm.200812-1943OC>.
34. Kukavica-Ibrulj I, Facchini M, Cigana C, Levesque RC, Bragonzi A. 2014. Assessing *Pseudomonas aeruginosa* virulence and the host response using murine models of acute and chronic lung infection. *Methods Mol Biol* 1149:757–771. http://dx.doi.org/10.1007/978-1-4939-0473-0_58.
35. Sambrook J, Fritsch EF, Maniatis T. 1989. Molecular cloning: a laboratory manual. Cold Spring Harbor Laboratory, Cold Spring Harbor, NY.
36. Visca P, Ciervo A, Sanfilippo V, Orsi N. 1993. Iron-regulated salicylate synthesis by *Pseudomonas* spp. *J Gen Microbiol* 139:1995–2001. <http://dx.doi.org/10.1099/00221287-139-9-1995>.
37. Ohman DE, Sadoff JC, Iglewski BH. 1980. Toxin A-deficient mutants of *Pseudomonas aeruginosa* PA103: isolation and characterization. *Infect Immun* 28:899–908.
38. Carmi R, Carmeli S, Levy E, Gough FJ. 1994. (+)-(S)-Dihydroaeruginoinic acid, an inhibitor of *Septoria tritici* and other phytopathogenic fungi and bacteria, produced by *Pseudomonas fluorescens*. *J Nat Prod* 57:1200–1205. <http://dx.doi.org/10.1021/np50111a002>.
39. Hoang TT, Karkhoff-Schweizer RR, Kutchma AJ, Schweizer HP. 1998. A broad host-range FLP-FRT recombination system for site-specific excision of chromosomally located DNA sequences: application for isolation of unmarked *Pseudomonas aeruginosa* mutants. *Gene* 212:77–86. [http://dx.doi.org/10.1016/S0378-1119\(98\)00130-9](http://dx.doi.org/10.1016/S0378-1119(98)00130-9).
40. Milton DL, O'Toole R, Horstedt P, Wolf-Watz H. 1996. Flagellin A is essential for the virulence of *Vibrio anguillarum*. *J Bacteriol* 178:1310–1319.
41. Schweizer HP. 1991. *Escherichia-Pseudomonas* shuttle vectors derived from pUC18/19. *Gene* 97:109–121. [http://dx.doi.org/10.1016/0378-1119\(91\)90016-5](http://dx.doi.org/10.1016/0378-1119(91)90016-5).
42. Hoang TT, Kutchma AJ, Becher A, Schweizer HP. 2000. Integration-proficient plasmids for *Pseudomonas aeruginosa*: site-specific integration and use for engineering of reporter and expression strains. *Plasmid* 43:59–72. <http://dx.doi.org/10.1006/plas.1999.1441>.
43. Antunes LC, Imperi F, Minandri F, Visca P. 2012. *In vitro* and *in vivo* antimicrobial activities of gallium nitrate against multidrug-resistant *Acinetobacter baumannii*. *Antimicrob Agents Chemother* 56:5961–5970. <http://dx.doi.org/10.1128/AAC.01519-12>.
44. Gaines JM, Carty NL, Colmer-Hamood JA, Hamood AN. 2005. Effect of static growth and different levels of environmental oxygen on *toxA* and *ptxR* expression in the *Pseudomonas aeruginosa* strain PAO1. *Microbiology* 151:2263–2275. <http://dx.doi.org/10.1099/mic.0.27754-0>.
45. Imperi F, Putignani L, Tiburzi F, Ambrosi C, Cipollone R, Ascenzi P, Visca P. 2008. Membrane-association determinants of the omega-amino acid monooxygenase PvdA, a pyoverdine biosynthetic enzyme from *Pseudomonas aeruginosa*. *Microbiology* 154:2804–2813. <http://dx.doi.org/10.1099/mic.0.2008/018804-0>.
46. James HE, Beare PA, Martin LW, Lamont IL. 2005. Mutational analysis of a bifunctional ferrisiderophore receptor and signal-transducing protein from *Pseudomonas aeruginosa*. *J Bacteriol* 187:4514–4520. <http://dx.doi.org/10.1128/JB.187.13.4514-4520.2005>.
47. Zhang S, Chen Y, Potvin E, Sanschagrin F, Levesque RC, McCormack FX, Lau GW. 2005. Comparative signature-tagged mutagenesis identifies *Pseudomonas* factors conferring resistance to the pulmonary collectin SP-A. *PLoS Pathog* 1:259–268.
48. Visca P, Colotti G, Serino L, Verzili D, Orsi N, Chiancone E. 1992. Metal regulation of siderophore synthesis in *Pseudomonas aeruginosa* and functional effects of siderophore-metal complexes. *Appl Environ Microbiol* 58:2886–2893.

49. Visaggio D, Pasqua M, Bonchi C, Kaever V, Visca P, Imperi F. 2015. Cell aggregation promotes pyoverdine-dependent iron uptake and virulence in *Pseudomonas aeruginosa*. *Front Microbiol* 6:902. <http://dx.doi.org/10.3389/fmicb.2015.00902>.
50. Imperi F, Tiburzi F, Fimia GM, Visca P. 2010. Transcriptional control of the *pvdS* iron starvation sigma factor gene by the master regulator of sulfur metabolism CysB in *Pseudomonas aeruginosa*. *Environ Microbiol* 12: 1630–1642. <http://dx.doi.org/10.1111/j.1462-2920.2010.02210.x>.
51. Caballero AR, Moreau JM, Engel LS, Marquart ME, Hill JM, O'Callaghan RJ. 2001. *Pseudomonas aeruginosa* protease IV enzyme assays and comparison to other *Pseudomonas* proteases. *Anal Biochem* 290: 330–337. <http://dx.doi.org/10.1006/abio.2001.4999>.
52. Miller JH. 1972. Experiments in molecular genetics. Cold Spring Harbor Laboratory, Cold Spring Harbor, NY.
53. Lee KM, Go J, Yoon MY, Park Y, Kim SC, Yong DE, Yoon SS. 2012. Vitamin B₁₂-mediated restoration of defective anaerobic growth leads to reduced biofilm formation in *Pseudomonas aeruginosa*. *Infect Immun* 80: 1639–1649. <http://dx.doi.org/10.1128/IAI.06161-11>.
54. King P, Citron DM, Griffith DC, Lomovskaya O, Dudley MN. 2010. Effect of oxygen limitation on the in vitro activity of levofloxacin and other antibiotics administered by the aerosol route against *Pseudomonas aeruginosa* from cystic fibrosis patients. *Diagn Microbiol Infect Dis* 66:181–186. <http://dx.doi.org/10.1016/j.diagmicrobio.2009.09.009>.
55. Konings AF, Martin LW, Sharples KJ, Roddam LF, Latham R, Reid DW, Lamont IL. 2013. *Pseudomonas aeruginosa* uses multiple pathways to acquire iron during chronic infection in cystic fibrosis lungs. *Infect Immun* 81:2697–2704. <http://dx.doi.org/10.1128/IAI.00418-13>.
56. Ankenbauer R, Sriyosachati S, Cox CD. 1985. Effects of siderophores on the growth of *Pseudomonas aeruginosa* in human serum and transferrin. *Infect Immun* 49:132–140.
57. Bonchi C, Frangipani E, Imperi F, Visca P. 2015. Pyoverdine and proteases affect the response of *Pseudomonas aeruginosa* to gallium in human serum. *Antimicrob Agents Chemother* 59:5641–5646. <http://dx.doi.org/10.1128/AAC.01097-15>.
58. Leoni L, Ciervo A, Orsi N, Visca P. 1996. Iron-regulated transcription of the *pvdA* gene in *Pseudomonas aeruginosa*: effect of Fur and PvdS on promoter activity. *J Bacteriol* 178:2299–2313.
59. Ochsner UA, Johnson Z, Lamont IL, Cunliffe HE, Vasil ML. 1996. Exotoxin A production in *Pseudomonas aeruginosa* requires the iron-regulated *pvdS* gene encoding an alternative sigma factor. *Mol Microbiol* 21:1019–1028. <http://dx.doi.org/10.1046/j.1365-2958.1996.481425.x>.
60. Schaible UE, Kaufmann SH. 2004. Iron and microbial infection. *Nat Rev Microbiol* 2:946–953. <http://dx.doi.org/10.1038/nrmicro1046>.
61. Sriyosachati S, Cox CD. 1986. Siderophore-mediated iron acquisition from transferrin by *Pseudomonas aeruginosa*. *Infect Immun* 52:885–891.
62. Xiao R, Kisaalita WS. 1997. Iron acquisition from transferrin and lactoferrin by *Pseudomonas aeruginosa* pyoverdine. *Microbiology* 143:2509–2515. <http://dx.doi.org/10.1099/00221287-143-7-2509>.
63. Hare NJ, Soe CZ, Rose B, Harbour C, Codd R, Manos J, Cordwell SJ. 2012. Proteomics of *Pseudomonas aeruginosa* Australian epidemic strain 1 (AES-1) cultured under conditions mimicking the cystic fibrosis lung reveals increased iron acquisition via the siderophore pyochelin. *J Proteome Res* 11:776–795. <http://dx.doi.org/10.1021/pr200659h>.
64. Dhooche B, Noël S, Huaux F, Leal T. 2014. Lung inflammation in cystic fibrosis: pathogenesis and novel therapies. *Clin Biochem* 47:539–546. <http://dx.doi.org/10.1016/j.clinbiochem.2013.12.020>.
65. Reid DW, Carroll V, O'May C, Champion A, Kirov SM. 2007. Increased airway iron as a potential factor in the persistence of *Pseudomonas aeruginosa* infection in cystic fibrosis. *Eur Respir J* 30:286–292. <http://dx.doi.org/10.1183/09031936.00154006>.
66. Smith DJ, Lamont IL, Anderson GJ, Reid DW. 2013. Targeting iron uptake to control *Pseudomonas aeruginosa* infections in cystic fibrosis. *Eur Respir J* 42:1723–1736. <http://dx.doi.org/10.1183/09031936.00124012>.
67. Moreau-Marquis S, Bomberger JM, Anderson GG, Swiatecka-Urban A, Ye S, O'Toole GA, Stanton BA. 2008. The DeltaF508-CFTR mutation results in increased biofilm formation by *Pseudomonas aeruginosa* by increasing iron availability. *Am J Physiol Lung Cell Mol Physiol* 295:L25–L37. <http://dx.doi.org/10.1152/ajplung.00391.2007>.
68. De Vos D, De Chial M, Cochez C, Jansen S, Tümmler B, Meyer JM, Cornelis P. 2001. Study of pyoverdine type and production by *Pseudomonas aeruginosa* isolated from cystic fibrosis patients: prevalence of type II pyoverdine isolates and accumulation of pyoverdine-negative mutations. *Arch Microbiol* 175:384–388. <http://dx.doi.org/10.1007/s002030100278>.
69. Jiricny N, Molin S, Foster K, Diggle SP, Scanlan PD, Ghoul M, Johansen HK, Santorelli LA, Popat R, West SA, Griffin AS. 2014. Loss of social behaviours in populations of *Pseudomonas aeruginosa* infecting lungs of patients with cystic fibrosis. *PLoS One* 9:e83124. <http://dx.doi.org/10.1371/journal.pone.0083124>.
70. Andersen SB, Marvig RL, Molin S, Krogh Johansen H, Griffin AS. 2015. Long-term social dynamics drive loss of function in pathogenic bacteria. *Proc Natl Acad Sci U S A* 112:10756–10761. <http://dx.doi.org/10.1073/pnas.1508324112>.
71. Hunter RC, Asfour F, Dingemans J, Osuna BL, Samad T, Malfroot A, Cornelis P, Newman DK. 2013. Ferrous iron is a significant component of bioavailable iron in cystic fibrosis airways. *mBio* 4:e00557-13. <http://dx.doi.org/10.1128/mBio.00557-13>.
72. Worlitzsch D, Tarran R, Ulrich M, Schwab U, Cekici A, Meyer KC, Birrer P, Bellon G, Berger J, Weiss T, Botzenhart K, Yankaskas JR, Randell S, Boucher RC, Döring G. 2002. Effects of reduced mucus oxygen concentration in airway *Pseudomonas* infections of cystic fibrosis patients. *J Clin Invest* 109:317–325. <http://dx.doi.org/10.1172/JCI0213870>.
73. Cao J, Woodhall MR, Alvarez J, Cartron ML, Andrews SC. 2007. EfeUOB (YcdNOB) is a tripartite, acid-induced and CpxAR-regulated, low-pH Fe²⁺ transporter that is cryptic in *Escherichia coli* K-12 but functional in *E. coli* O157:H7. *Mol Microbiol* 65:857–875. <http://dx.doi.org/10.1111/j.1365-2958.2007.05802.x>.
74. Koch D, Chan AC, Murphy ME, Lilie H, Grass G, Nies DH. 2011. Characterization of a dipartite iron uptake system from uropathogenic *Escherichia coli* strain F11. *J Biol Chem* 286:25317–25330. <http://dx.doi.org/10.1074/jbc.M111.222745>.
75. Brickman TJ, Armstrong SK. 2012. Iron and pH-responsive FtrABCD ferrous iron utilization system of *Bordetella* species. *Mol Microbiol* 86: 580–593. <http://dx.doi.org/10.1111/mmi.12003>.
76. Gi M, Lee KM, Kim SC, Yoon JH, Yoon SS, Choi JY. 2015. A novel siderophore system is essential for the growth of *Pseudomonas aeruginosa* in airway mucus. *Sci Rep* 5:14644. <http://dx.doi.org/10.1038/srep14644>.
77. Marvig RL, Damkier S, Khademi SM, Markussen TM, Molin S, Jelsbak L. 2014. Within-host evolution of *Pseudomonas aeruginosa* reveals adaptation toward iron acquisition from hemoglobin. *mBio* 5:e00966-14. <http://dx.doi.org/10.1128/mBio.00966-14>.
78. Nguyen AT, O'Neill MJ, Watts AM, Robson CL, Lamont IL, Wilks A, Oglesby-Sherrouse AG. 2014. Adaptation of iron homeostasis pathways by a *Pseudomonas aeruginosa* pyoverdine mutant in the cystic fibrosis lung. *J Bacteriol* 196:2265–2276. <http://dx.doi.org/10.1128/JB.01491-14>.
79. Peters BM, Jabra-Rizk MA, O'May GA, Costerton JW, Shirtliff ME. 2012. Polymicrobial interactions: impact on pathogenesis and human disease. *Clin Microbiol Rev* 25:193–213. <http://dx.doi.org/10.1128/CMR.00013-11>.
80. Kaneko Y, Thoendel M, Olakanmi O, Britigan BE, Singh PK. 2007. The transition metal gallium disrupts *Pseudomonas aeruginosa* iron metabolism and has antimicrobial and antibiofilm activity. *J Clin Invest* 117:877–888. <http://dx.doi.org/10.1172/JCI30783>.
81. Wurst JM, Drake EJ, Theriault JR, Jewett IT, VerPlank L, Perez JR, Dandapani S, Palmer M, Moskowitz SM, Schreiber SL, Munoz B, Gulick AM. 2014. Identification of inhibitors of PvdQ, an enzyme involved in the synthesis of the siderophore pyoverdine. *ACS Chem Biol* 9:1536–1544. <http://dx.doi.org/10.1021/cb5001586>.
82. Frangipani E, Bonchi C, Minandri F, Imperi F, Visca P. 2014. Pyochelin potentiates the inhibitory activity of gallium on *Pseudomonas aeruginosa*. *Antimicrob Agents Chemother* 58:5572–5575. <http://dx.doi.org/10.1128/AAC.03154-14>.
83. Visca P, Bonchi C, Minandri F, Frangipani E, Imperi F. 2013. The dual personality of iron chelators: growth inhibitors or promoters? *Antimicrob Agents Chemother* 57:2432–2433. <http://dx.doi.org/10.1128/AAC.02529-12>.
84. Simon R, Priefer U, Puhler A. 1983. A broad host range mobilization system for *in vivo* genetic engineering: transposon mutagenesis in Gram-negative bacteria. *Biotechnology* 1:784–791. <http://dx.doi.org/10.1038/nbt1183-784>.